Research Square

Preprints are preliminary reports that have not undergone peer review.
They should not be considered conclusive, used to inform clinical practice,
or referenced by the media as validated information.

Posture-aware vibration measurement and health monitoring of a tilting-rotary spindle head: Experimental modal validation and PCA-GMM anomaly detection

Tzu-Chi Chan
National Formosa University
Lu Heng-Yu
National Formosa University
Aman Ullah
d1175105@nfu.edu.tw
National Formosa University https://orcid.org/0009-0000-6239-0874
Kai-Jung Chang
National Formosa University

Research Article

Keywords: Spindle health monitoring, Posture-dependent dynamics, Experimental modal analysis, Vibration measurement, Gaussian mixture model, Anomaly detection

Posted Date: November 23rd, 2026

DOI: https://doi.org/10.21203/rs.3.rs-11685223/v1

License: This work is licensed under a Creative Commons Attribution 4.0 International License.
Read Full License

Posture-aware vibration measurement and health monitoring of a tilting-rotary spindle head: Experimental modal validation and PCA-GMM anomaly detection

Tzu-Chi Chan[1], Lu Heng-Yu[1], Aman Ullah[*2], Kai- Jung Chang[1]

[1]Department of Mechanical and Computer-Aided Engineering, National Formosa University, Huwei Township, Yunlin County 632, Taiwan
[2]Department of Power Mechanical, National Formosa University, Huwei Township, Yunlin County 632, Taiwan

Correspondence to: Aman Ullah / D1175105@nfu.edu.tw, amanullahshakir188@gmail.com

Abstract

Tilting-rotary spindle heads on multitasking machining centers exhibit swing-angle-dependent compliance and vibration, which posture-invariant measurement and monitoring schemes cannot capture. This study proposes a posture-aware framework that integrates finite element (FE) structural dynamics, impact-hammer experimental modal analysis (EMA), and unsupervised vibration-based health monitoring for an in-service spindle head at swing angles of 0°, 45°, and 90°. Static, modal, harmonic, and transient FE analyses under identical boundary conditions showed that global maximum deformation varied slightly (6.28-6.41 μm), whereas tool-point deformation reached 4.82 μm at 90° versus 4.44 μm at 0°, indicating that global stiffness inadequately represents machining compliance. The first two natural frequencies remained within 217-231 Hz without mode switching. Impact-hammer EMA with 30 measurement points and a triaxial accelerometer at 0° and 90° agreed with the FE predictions within 8.3%. Building on this validated posture dependence, a posture-stratified diagnostic scheme was developed. Ten 256 Hz frequency-band features and statistical time-domain features were extracted from 1 s windows of the Y-axis vibration signal and projected by principal component analysis (PCA). A Gaussian mixture model (GMM) trained exclusively on healthy data served as the baseline, requiring neither fault labels nor predefined thresholds. In proof-of-concept tests at 3500 rpm idle running, healthy features formed compact clusters at all three postures, whereas the abnormal state, induced by controlled rubber-mallet impacts, produced dispersed features that shifted away from the healthy baseline, with the degree of separation depending on posture. These results support posture-conditioned vibration measurement and anomaly detection for smart maintenance of multitasking machine tools.

Keywords: Spindle health monitoring; Posture-dependent dynamics; Experimental modal analysis; Vibration measurement; Gaussian mixture model; Anomaly detection

1. Introduction

Angle dependent vibration and stiffness uncertainties in the case of the tilting-rotary spindle head are considered critical because they are prone to failure within the boundaries of high precision multi-tasking machining. Lack of posture-aware models and the inability to validate these models through experiments are considered significant limitations for spindle designs and predictive maintenance [1-3]. The basics of spindle work have successfully outlined a systematic and component specific comprehension of modern spindle units and their interrelated thermo mechanical dynamics, emphasizing spindle dynamics as a unified process chain instead of considering individual sub-components[1, 2]. On the other hand, operational modal analysis has appeared to be a feasible technique for determining dynamic parameters in realistic machining tasks beyond the bounds of traditional impact test methods and allowing for characterization in a range of spindle speed and cutting conditions [4, 5]. Experimental identification for rotating spindle tool dynamics has already confirmed that precise modal identification still requires a preferential measurement strategy in a possibly appropriate test layout for effective operational modes relevant to machinability [6]. In recent decades, work efforts have been highly focused on the evaluation and representation of geometric errors in five axis machining centre models. Innovative identification methods, based on the simultaneous control of three and four axes, have been developed to analyse the systematic geometric errors characteristic of those machine models designed with a tilting rotary table approach [7, 8]. Experimental verification of system accuracy has also been carried out utilizing telescoping magnetic ball bars as test modalities for determination of system accuracy levels [9]. Through this background, Mayer et al.[10, 11] have developed theoretical and numerical models concerning link geometric deviation identification for machine models of five axes using methodologies based on telescoping ball bars. For their part, other work have analysed

integral error modeling and measurement methods for machine models of the tilting rotary table kind for their specific machine models[12].

The stiffness and dynamics of machine tool components are closely allied to machining precision and are especially important in advanced multifunctional machining centers [6, 13, 14]. In tilting-rotating spindle heads, changes in swinging position increase load paths, boundary conditions, and vibration characteristics of the spindle system, and therefore may induce position dependent deformations and natural frequencies. These factors increase resonance and vibration related precision degradation issues in machining and are therefore important considerations in making reliable assessments of spindle system behavior at various angles. FEA has been widely used in investigating static and dynamic characteristics of machine tool structures [15-17]. However, results obtained through numerical analysis are inevitably fraught with certain inherent uncertain-ties in modeling, discretization, contact, and boundary conditions. Therefore, modal analysis or operational deflection shapes have come to be accepted as essential methodologies in validating results on machine tool structures and accurately ascertaining natural modes and corresponding natural frequencies in real operating scenarios[18, 19] . Apart from structural features, vibration signals from spindle units provide considerable data for diagnosis and monitoring. Current investigations have confirmed the effectiveness of data-driven diagnostic approaches encompassing spectral threshold monitoring [20], supervised classification frameworks [21], and unsupervised dimensionality-reduction methods such as PCA-based anomaly detection [22, 23] for spindle fault identification; however, these methods universally presuppose mechanical stationary and therefore fail to account for the posture dependent structural dynamics inherent to tilting rotary spindle configurations. However, most current diagnosis models do not take into consideration posture dependent structural dynamics and therefore are not applicable to tilted and rotary spindle units for all possible working positions. With these challenges in mind, the aim of this study is to set up a posture conscious and experimentally validated investigation framework for tilting-rotary spindle heads of multi-tasking machining centers. Through the integration of static, modal, transient, and harmonic analyses with the use of experimental modal analysis, operational deflection shape analysis, and predictive diagnostics that utilize principal component analysis, the study hopes to fill the gap that currently exists between numerical analysis and experimental verification and the application of advanced diagnostics.

The study makes innovative and technical progress in the area of structural analysis and smart diagnosis of multi-tasking machining centers with tilting rotary spindle heads. The major points include are posture sensitive examination of the spindle head's dynamics. Our work involves evaluating a tilting rotary spindle head at swing angles of 0°, 45°, and 90°. In fact, through a detailed analysis of static deformation, modal analysis, harmonic analysis, and transient analysis, it will be made clear how a swing angle affects spindle head stiffness and dynamic behavior because current approaches often model a spindle at one swing angle. A high-fidelity Finite Element (FE) model of multi-posture spindles is also developed and its validation is carried out by combining EMA and operational deflection shapes. The consistency existing between the numerical results for natural frequencies, mode shapes, and experimental values confirms the validation of the proposed model and its suitability for posture dependent dynamics analysis. Experimental validation is conducted to confirm the consistency between numerical predictions and physical measurements across multiple swing orientations. Contrary to validating simulations at one posture, we assess consistency at various swing angles. The results demonstrate that the dynamic characteristics of the intermediate posture 45° fall progressively between those of the two extreme configurations 0° and 90°, providing experimental evidence of posture-dependent and continuously varying structural behavior. Unlike existing diagnostic methods that treat the spindle as a posture-invariant mechanical system, the proposed PDPS embeds experimentally validated, posture dependent structural dynamics as an explicit physical conditioning layer within a GMM-augmented PCA-based diagnostic architecture, thereby enabling threshold free, annotation free health assessment across the complete operational swing range of the tilting-rotary spindle head, a capability unreported in the existing spindle condition monitoring works. Thus, diagnosis can be made effectively for both normal and faulty conditions for all postures, thereby extending the conventional condition monitoring technique to variable spindle postures. An integrated posture-aware framework is presented for machining accuracy assessment and predictive maintenance of multi-tasking machining centers equipped with tilting-rotary spindle heads. Through the integration of FEA, experimental validation, and data-driven diagnosis within a single posture aware system, this study offers a method for mitigating the risk of resonance, enhancing the accuracy of machining, and carrying out predictive maintenance for multi-tasking machines with a tilting-rotary spindle head.

The rest of the paper is divided as follows: Section 2 introduces the multi-tasking machining center and the tilting and rotary spindle head being investigated from the context of FE modeling performed with descriptions of the material properties and boundary settings to be considered. Section 3 provides the results of the analysis

conducted with definitions of static deformation analysis, mode shape analysis, harmonic analysis, and transient analysis at each swing angle. Section 4 describes the validation of the analysis performed from the experimentation conducted to measure the deflection shapes of the machining center during operation with comparisons of the analysis and experiment results objectively quantified. Section 5 discusses the health monitoring of the machining center based on the analysis conducted with principal component analysis and provides the conclusion and suggestions for further studies in Section 6.

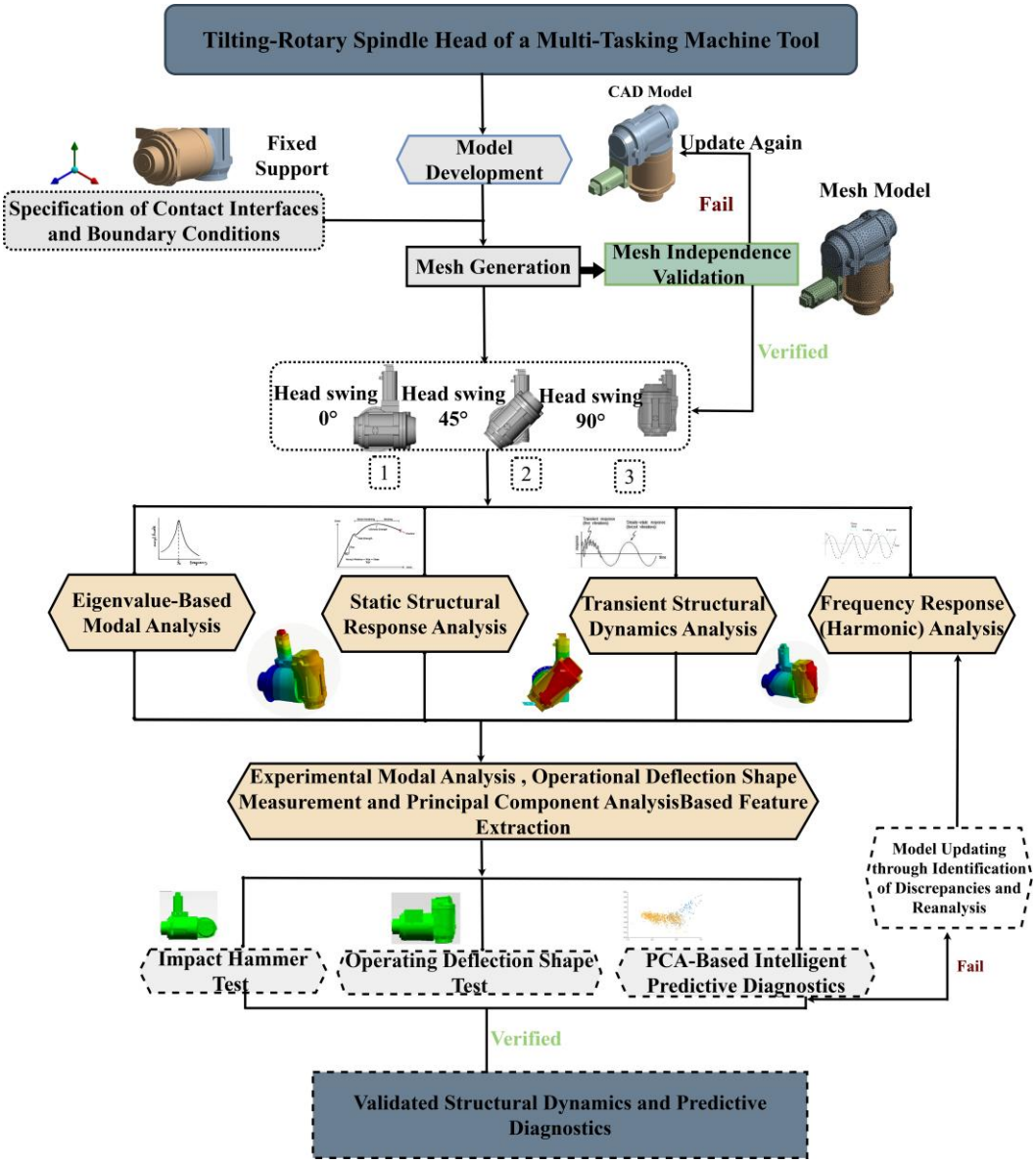

Fig. 1. Workflow posture dependent spindle analysis and predictive diagnostics

2. System description and Methodology

2.1. Numerical model of the multi-tasking machining center and tilting rotary spindle head

This study explores the tilting-rotary spindle head on the multi-tasking machining center shown in Figure 2 (a) INTEGREX i-200, which enables both turning and milling operations with the capability to perform multiple processes in one setup with reduced fixture changes, tool interchange, work handling, and noncutting time. The key specifications of the machining center are summarized in Table 1.

Table 1. Specification of machining center

Parameter	Specification

Chuck size	8 inch
Main spindle maximum speed	5,000 rpm
Milling spindle maximum speed	12,000 rpm
B-axis swing travel	240°

In order to observe posture-sensitive behavior, the tilting rotary swing spindle head is analyzed at model swing angles of 0°, 45°, and 90° as shown in Figure 2 (b-e) during the FEA and EMA.

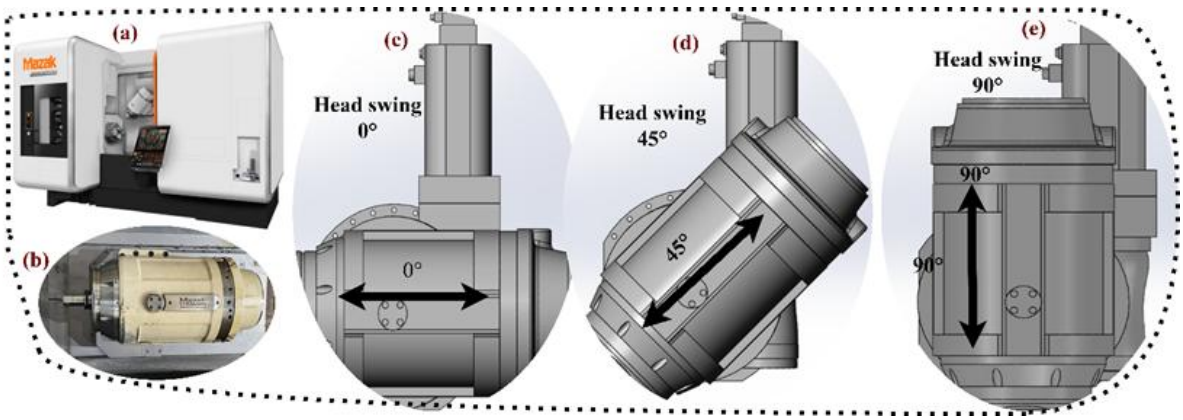

Fig. 2. Model development of the tilting-rotary spindle head: (a) INTEGREX i-200 multi-tasking machining center, (b) prototype used for experiment, and (c–e) tilting-rotary spindle head at swing angles of 0°, 45°, and 90°.

The model results for the tilting-rotary spindle head corresponded to a three-dimensional FE model developed in such a manner as to preserve global stiffness and characteristic dynamic properties. The original CAD assembly used in this model has been optimized by eliminating secondary geometries irrelevant for carrying loads and dynamic modes, thus precluding artificial stiffening of regions of interest through better mesh quality. In modelling the problem, all objects are considered as an isotropic homogeneous linear elastic body, S45C steel material being used for their realization in order to provide material uniformity throughout the assembly shown in Table 2.

Table 2. Material properties of SCP10.

Young's modulus (GPa)	2.06×10^{11}
Poisson's ratio	0.3
Density (kg/ m^3)	7840

2.2. FEA Based Posture Analysis

To discretize space, second order tetrahedral elements were utilized to effectively capture the geometric curvature and mode shapes of deformations. A mesh independence study was conducted by monitoring the maximum self-weight induced deformation and mesh quality index as a function of element size, as shown in Figure 3. The results demonstrate that at a global element size of 20 mm, the deformation response reaches a stable value, with the relative variation between the 20 mm and the next refined mesh falling below 1%, satisfying the convergence criterion[24]:

$$\varepsilon = \frac{|u_n - u_{n+1}|}{u_n} \times 100\% < 1\%$$

where:

u_n = Maximum deformation at current mesh size, u_{n+1} = maximum deformation at next refined mesh size and ε = relative error between consecutive refinements. Further refinement below 20 mm yields negligible improvement in deformation accuracy while significantly reducing mesh quality index, confirming 20 mm as the optimal element size balancing solution accuracy and computational efficiency.

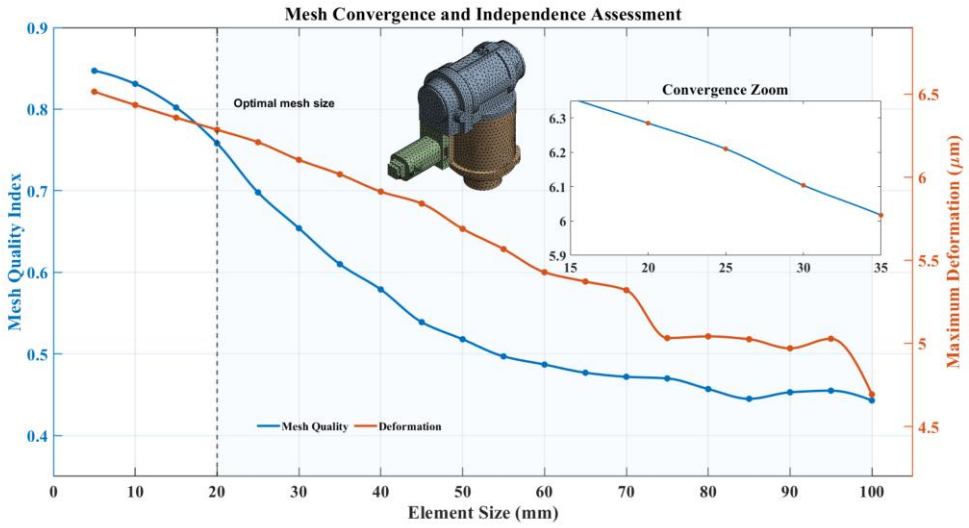

Fig. 3. Mesh convergence and independence assessment

The boundary conditions were specified such that it could replicate the mechanical constraint conditions existing in the spindle head during its operation. The interface where the spindle head is mounted onto the machine column was constrained fully. The loading conditions included the effect of gravity, and the same constraint conditions were applied during the modal, harmonic, and transient analyses. With a unified modeling approach, the analyses of static deformation, eigenfrequency, distribution, frequency response characteristics, and time domain dynamic response characteristics were made for spindle swing postures at angles of 0°, 45°, and 90°. In the analysis, the stiffness characteristics can be directly assessed irrespective of numerical and boundary condition discrepancies caused by postures.

2.3. Experimental and numerical modal analysis for structural dynamic validation

FEA is employed in this study to predict the natural frequencies and mode shapes of the tilting-rotary spindle head assembly across multiple swing postures[25]. The dynamic properties inherent to the tilting and rotary motion of the spindle head are investigated by Eigen value based modal analysis, where the modes of vibration are defined independent of any forcing function. The equation of motion for general linear elastic systems resolved into FE is given by [26, 27]. For instance, equation is used to calculate a response surface as follows:

$$\mathrm{M}\ddot{\mathrm{u}}(t) + \mathrm{C}\dot{\mathrm{u}}(t) + \mathrm{K}\mathrm{u}(t) = 0 \quad (1)$$

Where M, C, and K represent global mass, damping, and stiffness matrices, while u(t) is the nodal displacement vector. The damping is ignored in eigenfrequency, computations to determine structural eigen modes, resulting in:

$$\mathrm{M}\ddot{\mathrm{u}}(t) + \mathrm{K}\mathrm{u}(t) = 0 \quad (2)$$

Substituting for a harmonic solution of the form $\mathrm{u}(t) = \phi e^{i\omega t}$ the resulting equation for the generalized eigenvalue problem is:

$$(\mathrm{K} - \omega^2\mathrm{M})\phi = 0 \quad (3)$$

where ω is the natural circular frequency and ϕ is the corresponding mode shape vector. Non-trivial solutions exist only when:

$$\det(\mathrm{K} - \omega^2\mathrm{M}) = 0 \quad (4)$$

For the tilting-rotary spindle head, the changed effective constraint condition resulting from the swing position causes the stiffness distribution to become position dependent. As a result, the assembled stiffness matrix K is dependent on the swing angle, leading to variations in the obtained eigenfrequencies:

$$f_n = \frac{\omega_n}{2\pi} \quad (5)$$

Eigenvalue analysis was done using three sets of representative spindle swing angles of 0°, 45°, and 90°. The first three natural frequencies were obtained under identical boundary constraints, with full fixation at the spindle-column interface with gravity loading applied, ensuring that the results are directly comparable across all postures. The natural frequencies are summarized as follows:

0°Posture

$$f_1 = 217.8\ \mathrm{Hz}, f_2 = 230.2\ \mathrm{Hz}, f_3 = 357.2\ \mathrm{Hz} \quad (6)$$

45° Posture

$$f_1 = 220.9\ \text{Hz}, f_2 = 230.1\ \text{Hz}, f_3 = 358.2\ \text{Hz} \quad (7)$$

90° Posture

$$f_1 = 224.2\ \text{Hz}, f_2 = 227.7\ \text{Hz}, f_3 = 356.3\ \text{Hz} \quad (8)$$

There exists a distinct trend with respect to the posture. From 0° to 90°, the first natural frequency sees an increase of 6.4 Hz, 2.94% with a notable effective stiffness increase corresponding to the dominant mode of deformation, which occurs in the first mode. There exists a moderate decrease of 2.5 Hz ,1.09% in the second mode, whereas the third mode only registers a marginal change of 0.9 Hz, 0.25% which indicates a higher level of stability with respect to the change in the posture which shown in Figure 4.

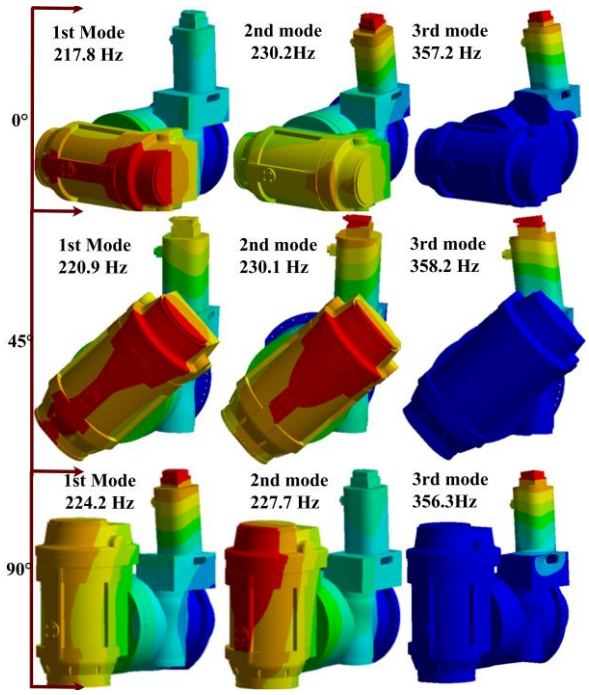

Fig. 4. First three mode shapes of the tilting-rotary spindle head at swing angles of 0°, 45°, and 90°

Mode shapes of tilting-rotary spindle head at 0°, 45°, and 90°. At 0°: the first mode 220.9 Hz corresponds to lateral swinging of the tilting spindle head in the X-axis direction; the second mode 230.1 Hz corresponds to lateral swinging in the Z-axis direction; the third mode 357.2 Hz corresponds to swinging of the spindle motor section in the X-axis direction. At 45°: the first mode 220.9 Hz involves coupled swinging in the X and Z-axis directions; the second mode 230.1 Hz involves coupled swinging in the Y and Z-axis directions; the third mode 358.2 Hz corresponds to swinging of the spindle motor section in the X-axis direction. At 90°: the first mode 224.2 Hz corresponds to swinging in the Z-axis direction; the second mode 227.7 Hz corresponds to swinging in the X-axis direction; the third mode 356.3 Hz corresponds to swinging of the spindle motor section in the X-axis direction. The mode shapes obtained are independent of the swing angles, with no mode switch observed in the first three modes, thereby implying that the frequency variation is dominated by stiffness variation due to the effect of the posture. These modes show the pattern distributions with respect to the rotation of the spindle head. In the first and second modes, the deflection pattern is dominated by the curvature of the spindle head assembly, which makes the modes more sensitive to the change in constraint orientation. In the third mode, the deflection pattern is more globally distributed, which makes the mode less sensitive to swing posture shown in Figure 5.

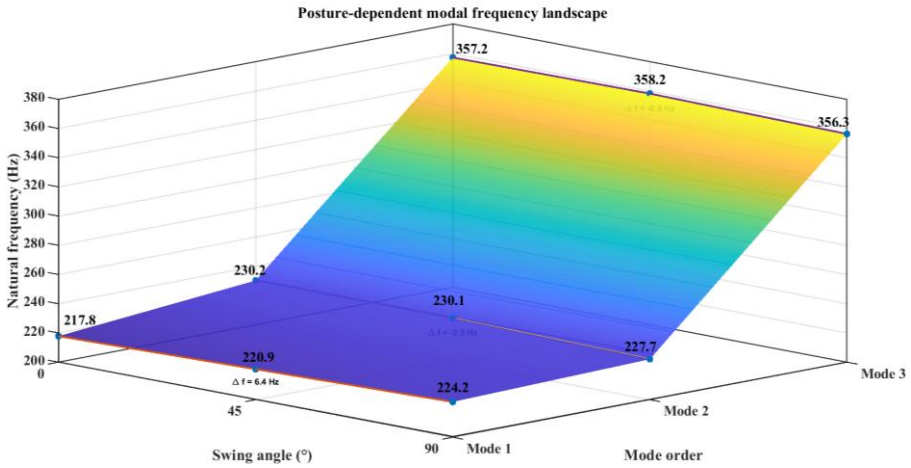

Fig. 5. Comparison of experimentally identified (EMA) and numerically predicted (FEA) natural frequencies

The three dimensional modal frequency map provides further insight into how swing angles are related to modal dynamics. Monotonic trend exists for the first mode where higher angles result in higher modal frequencies, whereas the other two modes show almost flat trends. Such trends hint at posture changes having significant impacts on lower order modes, which are most important in vibration suppression and resonance elimination in actual machining tasks. On the whole, the eigenvalue-based modal analysis shows that the spindle swing posture has a certain impact on the dynamics of the tilting rotary spindle head. This provides a basic foundation for the subsequent frequency response analysis and transient dynamics assessment, and is crucial for the posture conscious vibration reduction and prediction diagnostics in multi-tasking machining centers.

2.4. Experimental validation

Modal Analysis is a highly popular tool used for dynamic system characterization. The development of EMA techniques was inspired by studies in structure engineering fields [27, 28]. Besides modal parameters, EMA has been applied to finite element model updating [29, 30], structural health monitoring [31, 32], prediction of modal variation with structural variations [33], and load identification with known modal parameters[34, 35]. Experimental validation is performed to validate accuracy of predictions about the modal characteristics of a tilting and rotary spindle head by use of finite element models. An experimental modal analysis has been done by impact hammer testing, which allows identification of structural modes of low order. The motion of the structure is dictated by the linear equation of motion:

$$\mathrm{M}\ddot{u}(t) + \mathrm{C}\dot{u}(t) + \mathrm{K}u(t) = \mathrm{f}(t) \tag{9}$$

Where M, C, and K represent the global mass, damping, and stiffness matrices, respectively, and:

$$\mathrm{H}(\omega) = \frac{\mathrm{U}(\omega)}{\mathrm{F}(\omega)} \tag{10}$$

where H(ω) is the Frequency Response Function (FRF) of the structure, U(ω) is the Fourier transform of the measured vibration response, and F(ω) is the Fourier transform of the input excitation force applied by the impact hammer. In modal testing, modal parameters are identified from the Frequency Response Function (FRF), where X(ω) and F(ω) denote the Fourier transforms of the measured response and input force signals, respectively. An impact hammer was utilized to generate broadband impulse excitation of the spindle head structure. The force was directly measured by the force transducer present in the hammer. Response measurements have been recorded by accelerometers placed at high sensitivity locations. Low-mass modal accelerometers were used to minimize the effect of additional mass on the dynamic characteristics of the tested structure, thereby ensuring that the measured modal parameters accurately represent the unloaded structural behavior. Repeatability was also improved by signal averaging. Multiple impact excitations were performed with each test setup. The FRFs are obtained from the simultaneous measurement of the excitation force signal, acquired by the force transducer in the hammer head, and the vibration response signal, acquired by the accelerometers mounted on the structure, enabling identification of the dynamic characteristics and validation of the numerical modal analysis results. The technical specifications are listed in Table 3.

Table 3. Impact Hammer Specifications

Parameter	Unit	Specification
Operating temperature range	℃	-20~70
Nominal sensitivity	mV/N	0.2
Measurement force range	N	0 ~ 20,000

Frequency range with steel tip (-10 dB)	Hz	5,400
Resonance frequency	kHz	27
Time constant (nominal)	s	500
Hammer head mass	g	500
Hammer head diameter	mm	32
Hammer head length	mm	94
Handle length	mm	236
Electrical connector	-	BNC

A force window was applied to the hammer input channel (Ch1), and exponential windows were applied to the three accelerometer response channels (Ch2-Ch4), with channel sensitivities set to 0.198 mV/N and 103.9, 104.0, and 104.6 mV/g respectively, per manufacturer calibration. Excitation applied in the Y-axis direction. The three axis accelerometer used for response measurement was the Endevco Model 65-100, a compact piezoelectric (IEPE) sensor capable of simultaneously measuring acceleration in three axes. Measured time domain signals were converted to the frequency domain via Fast Fourier Transform (FFT) for vibration analysis across different frequency bands. The technical specifications are listed in Table 4.

Table 4. Accelerometer Specifications

Parameter	**Unit**	**Specification**
Measurement range	g (m/s^2)	$\pm 50(\pm 490)$
Voltage sensitivity (nominal)	$mV/g(mV/m/s^2)$	100 (10.2)
Amplitude response (± 1 **dB**)	Hz	1.5 ~ 6,000
Amplitude response (± 3 **dB**)	Hz	0.7 ~ 6,000
Phase response $(\pm 5^{\circ})$	Hz	10 ~ 1,500
Resonance frequency	Hz	45,000
Signal coupling	-	IEPE
X-axis sensitivity (calibrated)	mV/g	103.9
Y-axis sensitivity (calibrated)	mV/g	104.0
Z -axis sensitivity (calibrated)	mV/g	104.6

A total of 30 measurement points were distributed symmetrically across the tilting head assembly, referenced to the global coordinate system (X: horizontal, Y: fore-aft, Z: vertical). Measurement points were avoided near sheet metal covers, electrical cabinets, and pipelines to minimize extraneous noise. At each measurement point, three repeated hammer impacts were applied and the resulting FRFs were ensemble averaged the experimental step as shown in Figure 6.

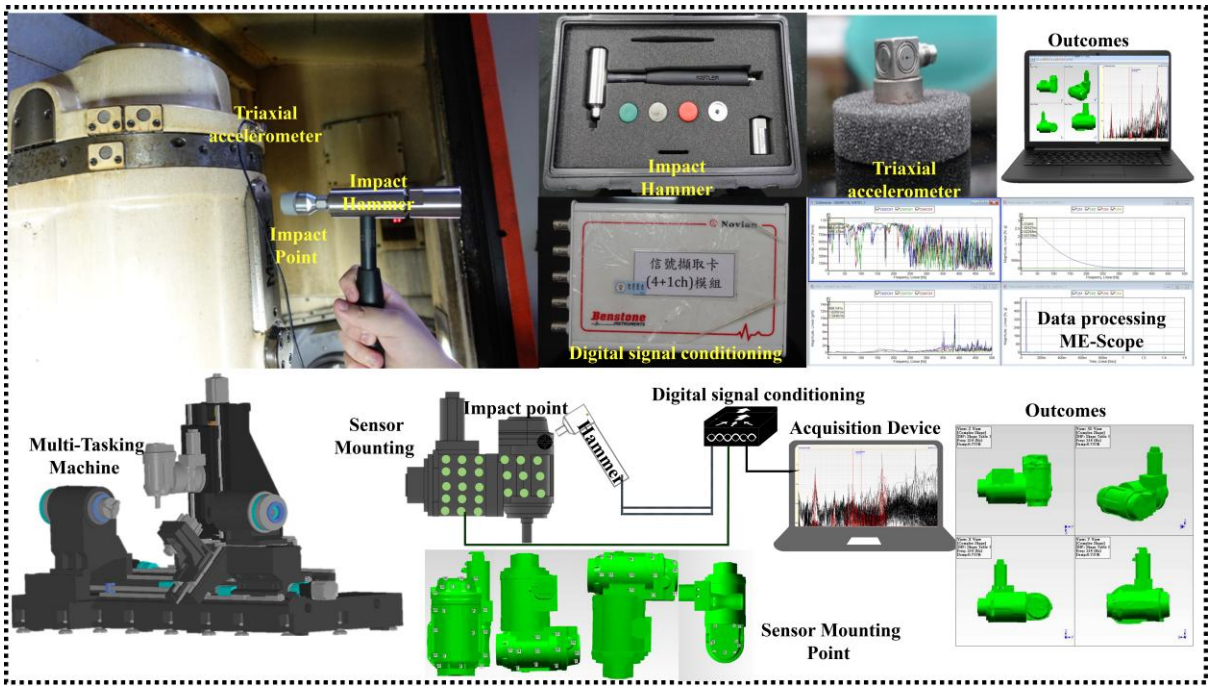

Fig. 6. Experimental setup for impact hammer testing

The forces and acceleration data were simultaneously measured utilizing a data acquisition system, and the inheritance frequency response functions were evaluated within the frequency domain. The curve fits of the measured frequency response functions were employed to extract the natural frequencies and their associated mode shapes, as shown in Figure 7.

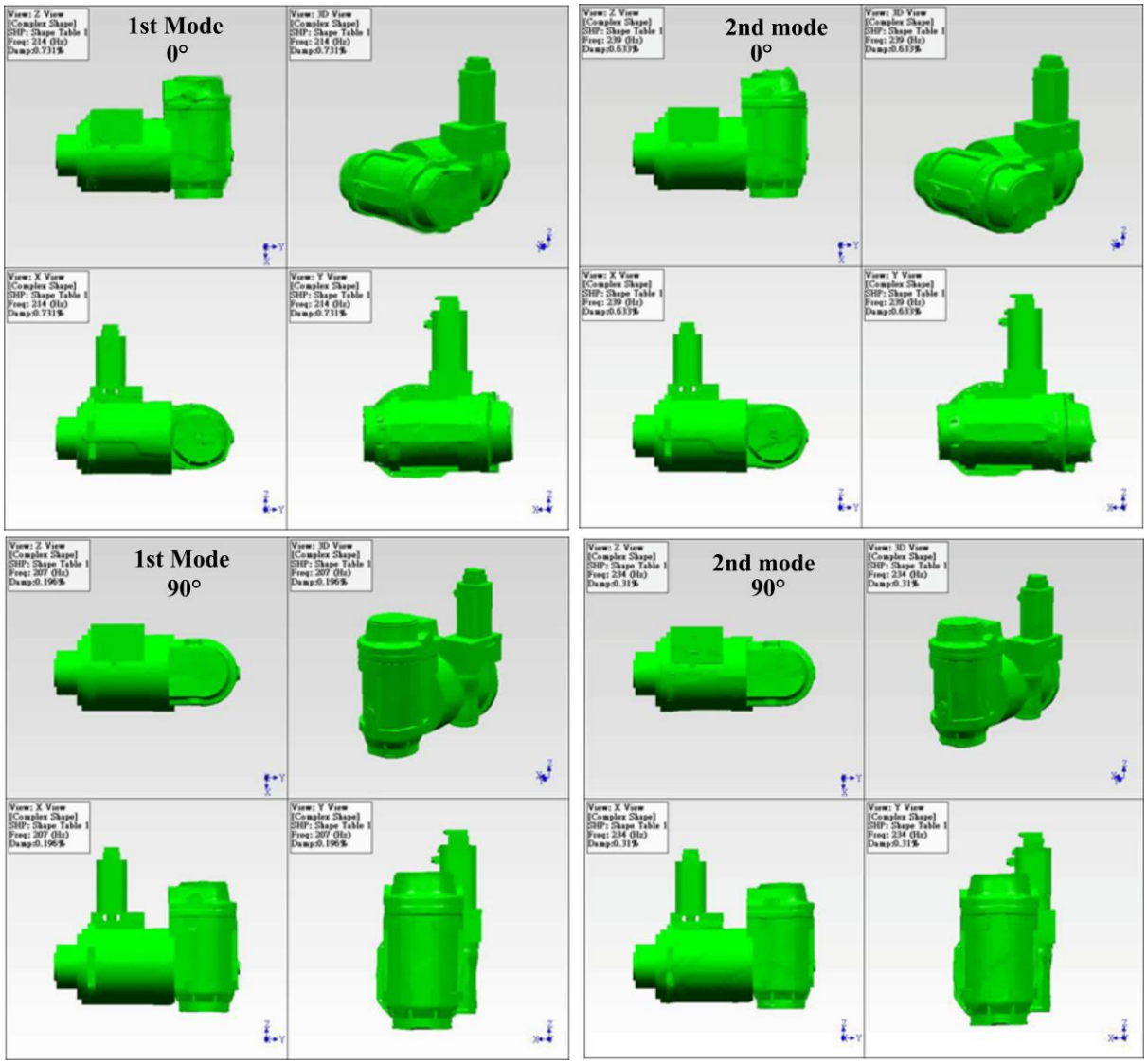

Fig. 7. Experimentally identified first two mode shapes and corresponding natural frequencies at swing angles of 0° and 90°.

In order to eliminate discrepancies between the numerical simulation and the experimental results, the spindle head was verified with the same boundary constraint conditions as those adopted in the finite element simulation. EMA performed at swing angles of 0° and 90° to validate the FEA predictions at the two extreme posture configurations. The results of the experimentally obtained natural frequencies were compared with the eigenfre quencies computed using the finite element method to check the numerical and experimental correlation. For the 0° pose, the first and second experimentally obtained natural frequencies were 214.0 Hz and 239.0 Hz, whereas the corresponding numerical values were 217.8 Hz and 230.2 Hz. The percentage deviation was 1.73% for the first mode and 3.84% for the second mode. For the 90° swing angle, the first natural frequency was 207.0 Hz (EMA) and 224.2 Hz (FEA), with a percentage difference of 7.66%; the second natural frequency was 234.0 Hz (EMA) and 227.7 Hz (FEA), with a percentage difference of 2.76%.The differences lie within the acceptable limit of ±10% in mode validation for a machine tool system, is shown in Figure 8.

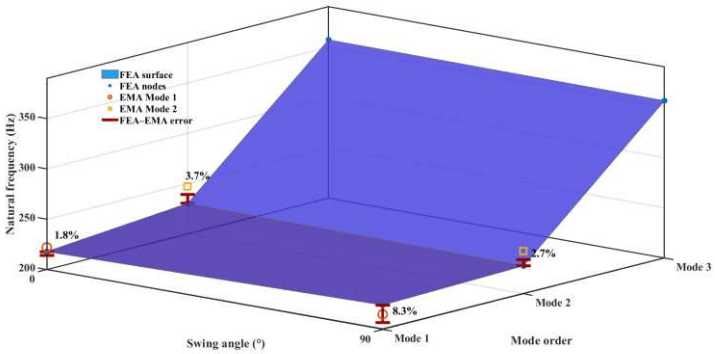

Fig. 8. Comparison of FEA and EMA natural frequencies and MAC matrix validation results at swing angles of 0° and 90°

The FEA to EMA frequency discrepancies were 1.8% and 3.7% for the first and second modes at 0°, and 8.3% and 2.76% at 90°. The FEA to ODS discrepancies were 5.71% and 1.39% at 0°, and 1.89% and 1.01% at 90°. All errors remained within the 10% acceptance threshold. MAC diagonal values approached unity for all identified mode pairs, confirming consistency between measured and predicted mode shapes.

3. Influence of swing orientation in static deformation behavior

Static structural analysis plays a crucial role in tilting-rotary spindle systems because posture and self-weight loading significantly influence overall stiffness and local deformation values around the cutting point, and this, in turn, affects machining accuracy. For this analysis, FEA simulation performed, considering self-weight loading with fixed contacts at the spindle and column interface to analyze values of deformation at swing angles of 0°, 45°, and 90°. From this analysis, it can be concluded that values of overall maximum deformation are concentrated around the spindle tip and vary negligibly with posture, measuring 6.41 µm at 0°, 6.32 µm at 45°, and 6.28 µm at 90°, with a total variation of less than 1 µm, indicating that swing angle variation exerts relatively minor influence on overall structural stiffness across all swing configurations, as shown in Figure 9.

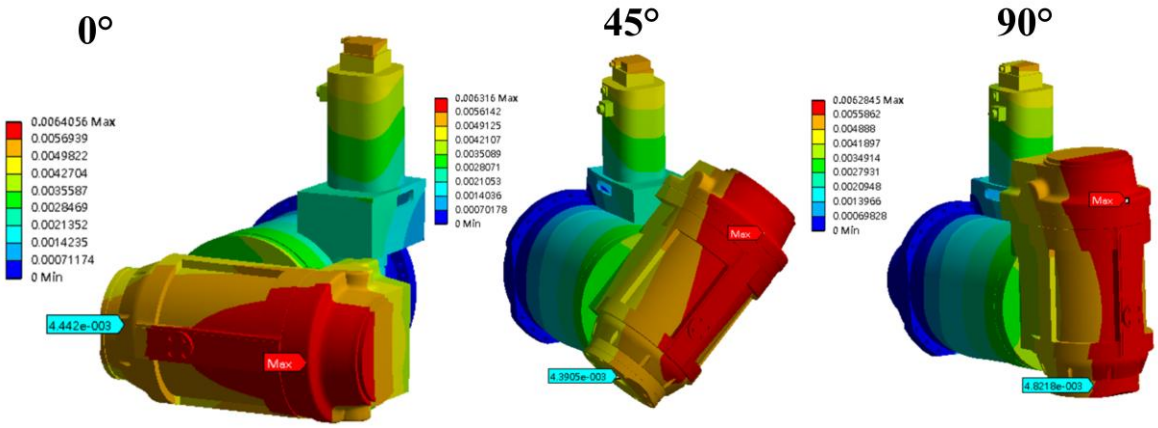

Fig. 9. FEA static deformation results of the tilting-rotary spindle head at swing angles of 0°, 45°, and 90°

However, analysis of values of deformation at the tool holder position draws significant variations based on posture change. Values of deformation at the tool holder position are 4.44 µm at 0° and 4.39 µm at 45°, which are comparable due to similar values of stiffness around the cutting interface, but at 90°, it measures 4.82 µm, which is higher due to the lower effective stiffness of the structure along the gravitational loading direction in this posture. At 0°, the self-weight acts predominantly along the spindle axis and is carried by an axially stiff load path, whereas at 90° the self-weight loads the overhung spindle head transversely, engaging a bending-dominated load path with lower effective stiffness at the tool point, which results in the larger tool-point deformation. This observation is consistent with the modal analysis results, in which the first natural frequency increases at 90°, because the modal stiffness is associated with a specific mode shape and vibration direction, whereas the static tool-point deformation is governed by the compliance along the direction of the gravitational load. These results demonstrate that the tool point deformation must be evaluated explicitly, as it serves as an application-oriented

stiffness measure that is more representative of machining accuracy than the global maximum deformation, which does not capture the posture-dependent compliance at the cutting interface

3.1. Posture Sensitive Frequency Response Characteristics and Resonance Mapping

The spectrum frequency response analysis is necessary for the tilting rotating spindle heads owing to the frequency dependence of the machining excitation. The identified posture-dependent resonant bands provide the basis for defining safe operational frequency ranges and for targeting vibration suppression in the vicinity of the structural resonance modes. Within the current investigation, the spectrum harmonic response analysis has been carried out by subjecting the spindle to the 300 N load located on the spindle front end. The frequency sweeping setup ranging between 1-700 Hz, while observing the corresponding spindle response measured along the X, Y, and Z-axes. The swing angles of 0°, 45°, and 90° as shown in Figure 10.

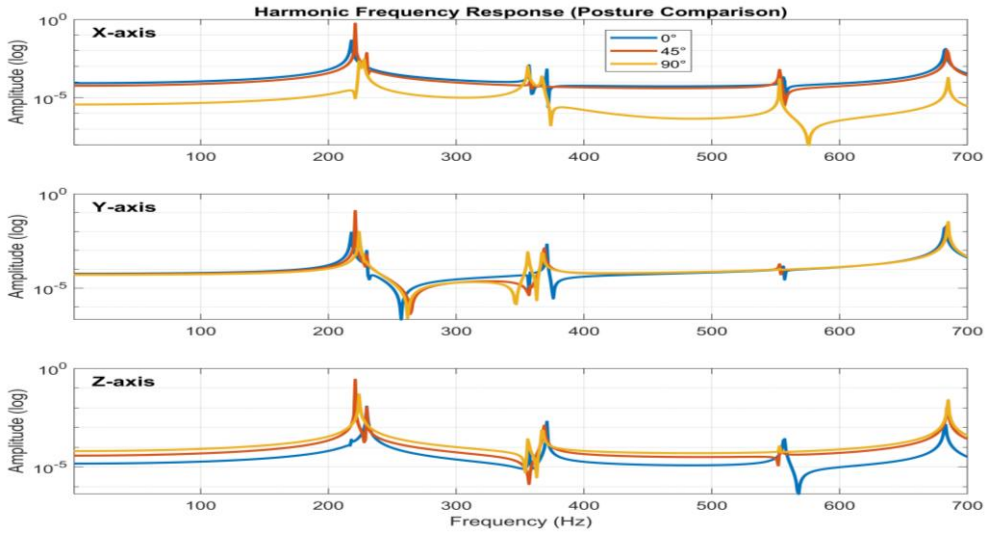

Fig. 10. Frequency response functions in the X, Y, and Z axes of the tilting-rotary spindle head at swing angles of 0°, 45°, and 90°.

The frequency response functions, hence derived, indicate significant response amplifications in the frequency bands corresponding to the modal values derived the modal analysis, thereby justifying the modal analysis results and confirming the equivalent dynamic stiffness model representation using the finite element model. Indeed, the main resonant bands lie in the frequency ranges corresponding to the first two modes, located at 217.8-230.2 Hz (0°), 220.9-230.1 Hz (45°), and 224.2-227.7 Hz (90°), whereas the high-frequency amplification is expected near the third mode located at 357.2 Hz (0°), 358.2 Hz (45°), and 356.3 Hz (90°). The minor shifts in the resonant frequency with the topological changes, however, clearly indicate the less significant swing-angle dependencies for the global dynamic stiffness, whereas the corresponding X, Y, and Z-AXISs FRFs indicate the application oriented mapping for the vibration sensitivity analysis necessary for the final posture selection for the spindle operational performance.

3.2. Time-Resolved Structural Response of the Tilting-Rotary Spindle

Transient structural analysis is required to understand the time-dependent deformation characteristics of the tilting-rotary spindle subjected to sudden force loading. For example, during tool workpiece engagement, inertial forces and modal superposition effects may produce transient deformations that exceed those predicted by static analysis alone. The analysis was performed in FEA transient structural with implicit time integration under identical conditions at all postures: full fixation at the spindle column interface, standard earth gravity, and a 300 N step force applied at the tool-holder contact area at t = 0.02 s, over a 1 s observation window with an output interval of 0.02 s. No explicit structural damping was assigned; the amplitude decay of the response is governed by the algorithmic damping of the implicit integration scheme at the employed time step. Under this loading, posture-dependent transient deformation levels of approximately 6.6 µm at 0°, 7.1 µm at 45°, and 6.4 µm at 90° were obtained, as shown in Figure 11.

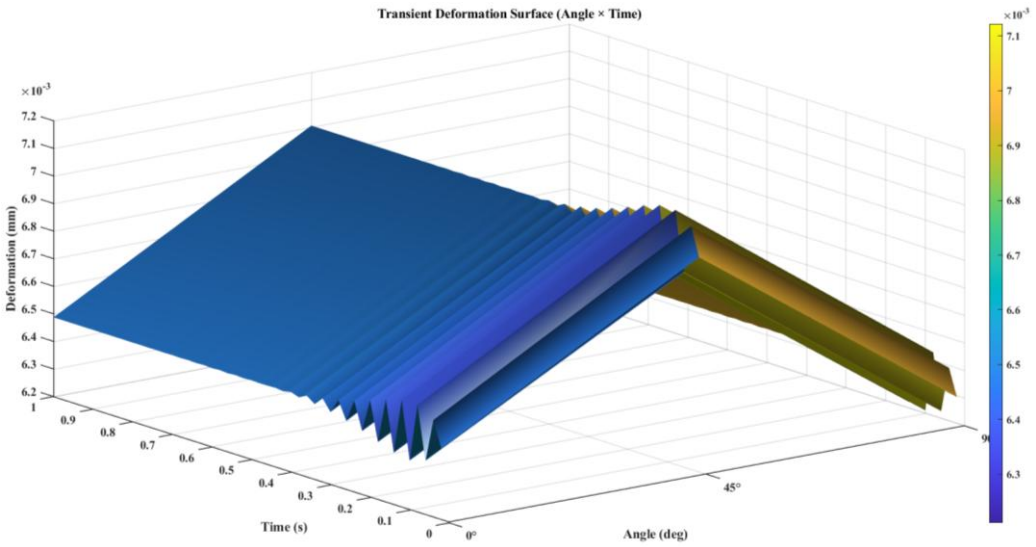

Fig.11. Time-resolved structural response at 0°, 45°, and 90°

In all posture configurations, the time-displacement plots show that steady-state convergence is achieved at approximately 0.4-0.5 s, within the 1 s total simulation duration, after which the response remains stable about the new equilibrium. The transient deformation is dominated by the gravitational preload, with the 300 N step load contributing an oscillatory increment of approximately ±0.1-0.15 µm about the equilibrium level. The transient analysis results show that the transient deformation level varies with posture, measuring approximately 6.6 µm at 0°, 7.1 µm at 45°, and 6.4 µm at 90°, while steady-state convergence is consistently achieved at approximately 0.5 s across all postures. This posture-dependent variation in transient deformation level provides a quantitative basis for posture selection in impact-sensitive machining operations, while the consistent 0.5 s settling time establishes a reliable time threshold for steady-state vibration signal acquisition in the PDPS diagnostic framework.

4. Predictive Diagnostic and Prognostic System (PDPS)

Existing spindle condition monitoring methodologies can be systematically classified into three principal categories. The first encompasses spectral threshold based approaches [20] wherein vibration amplitude or frequency domain indicators are compared against empirically calibrated limits; while interpretable, such methods are inherently configuration-specific and become structurally unreliable when the mechanical transfer function of the spindle varies with operating posture. The second category comprises supervised classification frameworks including support vector machines, convolutional neural networks, and gradient boosted classifiers [21] which demonstrate high discriminative accuracy under controlled conditions but require fault-annotated training datasets that are rarely obtainable in operational industrial environments and cannot generalize across structurally distinct postures without complete retraining. The third category encompasses unsupervised anomaly detection methods based on PCA residuals or reconstruction error [22, 23], which circumvent the labeling requirement but impose a posture-invariant unimodal Gaussian assumption on the feature space, rendering them insensitive to the systematic distributional shifts induced by swing-angle-dependent structural dynamics. The proposed PDPS departs fundamentally from all three categories. Rather than applying a single global diagnostic model, the PDPS conditions the diagnostic baseline explicitly on the posture-dependent structural dynamics established through FEA and EMA across three representative swing configurations. Within each posture stratified regime, PCA serves as a dimensionality reduction operator projecting the multidimensional vibration feature space onto its principal axes of variance, while a gaussian mixture model selected in preference to a unimodal Gaussian or fixed threshold to accommodate the multi modal feature distributions arising from distinct operational states characterizes the healthy baseline distribution. This posture-stratified, physics-informed, probabilistic modeling architecture, requiring neither fault annotated training data nor a priori threshold specification, constitutes the methodological novelty of the PDPS and represents an advancement unreported in the existing spindle health monitoring literature. The output signal from the accelerometer was connected to the DAQ204 four-channel data acquisition module (maximum sampling rate 102.4 kS/s, i.e., 102.4 kHz). Signals were acquired with an effective analysis bandwidth of 2560 Hz, corresponding to an effective sampling rate of 6.4 kS/s, with 6400 samples per acquisition window (1 s window length), yielding a frequency resolution of 1 Hz per bin. FFT-based spectral

features were partitioned into ten sub-bands of 256 Hz each, spanning the full 0-2560 Hz bandwidth, and together with statistical time-domain features formed the feature vector xi as defined in equation (11). Let x (t) represent the vibration signal collected from the spindle head. After signal segmentation, each vibration signal is translated into a feature vector:

$$\mathbf{x}_i = [x_{i1}, x_{i2}, \ldots, x_{iD}]^{\mathrm{T}} \tag{11}$$

where D represents the number of frequency domain and statistical features that have been derived from the vibration signal. Principal component analysis (PCA) is used for dimensionality reduction of the feature space, retaining the major variability information. The covariance matrix of the feature set is given by:

$$\mathrm{C} = \frac{1}{N}\sum_{i=1}^{N} (\mathrm{x}_i - \mu)(\mathrm{x}_i - \mu)^{\mathrm{T}} \tag{12}$$

where μ is the mean feature vector. Through eigenvalue decomposition of the matrix C, the feature vectors are projected into the lower-dimensional space:

$$\mathrm{z}_i = \mathrm{W}^{\mathrm{T}}(\mathrm{x}_i - \mu) \tag{13}$$

where W holds the principal eigenvectors. In the statistical distribution of the reduced features, a Gaussian mixture model is used:

$$p(\mathbf{z}) = \sum_{k=1}^{K} \pi_k \mathcal{N}(\mathrm{z} \mid \mu_k, \Sigma_k), \sum_{k=1}^{K} \pi_k = 1 \tag{14}$$

where πk, μk, and Σk are the weight, means, and covariances corresponding to the k-th Gaussian distribution component, and K is the total number of mixture components. In the PDPS framework, the health state is assessed from the dispersion of the vibration feature vectors in the PCA-reduced space relative to the healthy-baseline distribution modelled by the GMM. Under healthy operation, the features are strongly correlated and project onto a compact, densely clustered region; under abnormal operation, the feature correlation decreases and the points disperse, spreading beyond and migrating away from the healthy cluster. The distinction is therefore defined by the compactness versus dispersion of the feature distribution with respect to the healthy GMM baseline, which is established without any fault-labelled data. The experimental setup was designed to measure posture-dependent vibration characteristics of the spindle head to confirm the proposed model of PDPS. The experiments were performed in noncutting and idle running modes to separate structural dynamics independent of machining processes. Piezoelectric acceleration sensors were mounted on the spindle head casing at a fixed point, as shown in Figure 12(a-c). The BALT-1801B is a single-axis accelerometer (sensitivity: 250 mV/g, measurement range: ±40 g, AC-coupled); it was oriented to measure vibration in the Y-axis (fore-aft) direction at all three swing angles (0°, 45°, 90°). This direction was selected based on the FEA harmonic analysis results, which confirmed the Y-axis as the dominant vibration response direction across all posture configurations. This location was chosen such that the sensitivity to the spindle structural vibration was maximized, while the added mass was kept at a minimum. This point was kept fixed even while changing the swing postures.

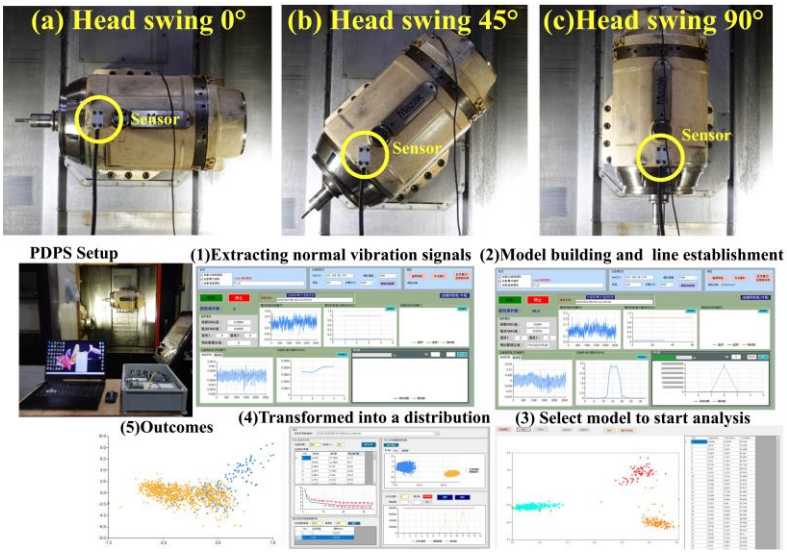

Fig.12. Experimental setup of Predictive Diagnostic and Prognostic System

The measurements were conducted on three different representative swing angles of the spindle 0°, 45°, and 90°, which are usually found in multi-tasking machine tools. The rotational speed of the spindle motor in each posture was set at 3500 rpm with stead state conditions. In this study, the healthy spindle state is defined as steady-state idle rotation at 3500 rpm, under which vibration signals exhibit periodic variation with stable amplitude. The abnormal state is defined as the condition induced by controlled rubber mallet impacts applied to the spindle body during idle rotation, which introduce transient impulsive force disturbances and produce spike amplitudes distinctly different from the healthy periodic baseline. These two states produce characteristically different vibration feature distributions: healthy features form a compact, tightly clustered region in the PCA-reduced feature space, while abnormal features exhibit a dispersed, scattered distribution migrating away from the healthy cluster boundary. The output signal from the accelerometer was connected to the PDPS data acquisition system, which recorded the vibration signals using the same parameters. The PDPS workflow, shown in Figure 12, includes the vibration acquisition which steady state vibration signals are captured continually from the spindle head. Signal segmentation work as raw signals are divided into samples of a fixed size, each considered a separate observation. Feature extraction utilized for frequency and statistical features are derived from the segment to produce a feature vector. PCA is applied to project the extracted feature vectors into a lower-dimensional space, after which Gaussian Mixture Models are trained exclusively on healthy baseline data to establish the reference distribution for anomaly detection. Health assessment is performed by analyzing new vibration patterns based on their distribution characteristics relative to the established baseline model. This allows real time health assessments based on posture independently of explicit fault annotations. In the PCA transformed 0° posture, the vibration behavior is shown to be a dense cluster under normal conditions, while a wider scatter is observed under abnormal conditions. This shows that there is a large variation in vibration under abnormal conditions and a lack of correlation between the variables. For 45°, both healthy and abnormal distributions remain focused around 45°, thus attesting that the PDPS space is not so sensitive to changes in moderate posture variations. However, variability in the abnormal distribution increases relative to that in 0° posture. In the case of a 90° angle, the abnormal distribution of features includes the highest variability. Number of feature points migrate towards the boundary area separating normal and abnormal regions, signifying the emergence of potentially abnormal areas where deterioration has started but not developed into unstable zones as yet. The outcomes show that the behavior of feature distribution has a dependable diagnostic capability for posture dependent spindle health as shown in Figure 13.

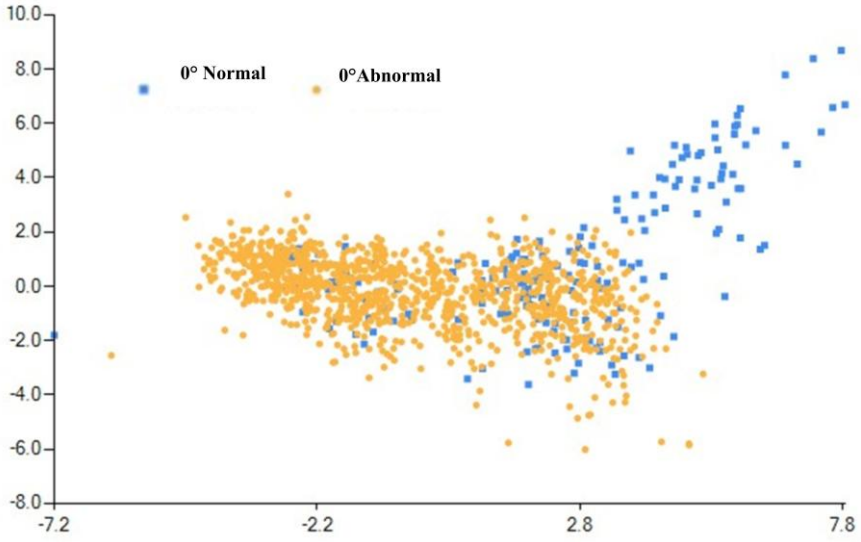

(a)

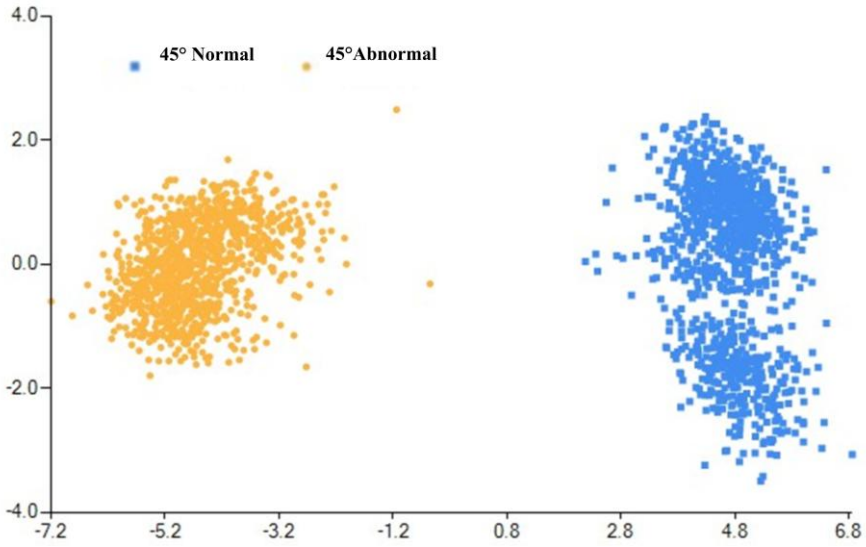

(b)

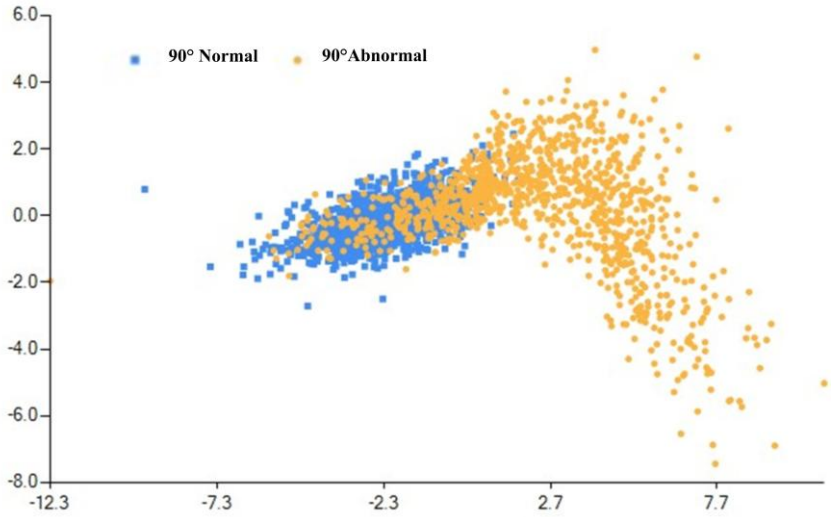

(c)

Fig. 13. Posture-dependent distribution of healthy and abnormal spindle vibration features at (b) 0°,(a) 45°, (c) and 90°

The posture-dependent variations in feature scatter and drift are consistent with the structural dynamic changes identified in the FEA and EMA results of the posture-dependent spindle model. The key importance of this fact finding work lies in combining posture-aware vibration signal acquisition techniques with a data driven diagnostic system that does not need any predefined threshold or explicit models for diagnosis. The proposed PDPS system has the ability to perform predictive health monitoring for a tilt-rotary spindle as well as provides a robust platform for intelligent maintenance of multi-tasking machine tools. This work combines the use of the finite element model based on the machine's posture, experimentally validated approaches, and predictive vibration analysis methods on a unified platform, with results confirming the natural vulnerability of the mechanical dynamics and health condition of the machine's spindle head modules to the machine's posture, irrespective of the machine's stiffness rigidity. The relationships and consistency observed across static deformation patterns, modal properties, frequency responses, transient settling responses. The distribution patterns of the diagnosed predictive vibration feature parameters justify the reported results by proving the intertwined relationship across structural mechanics properties and vibration patterns due to the swing orientation angle. In view of the explained interwoven relationship across structural mechanics properties and vibration patterns due to the swing orientation angle, the requirement for structural characterization methods based on the machine's posture is recognized as essential for accurate stiffness analysis, vibration analysis, and predictive health condition analysis for modern multi-tasking

machine tools. The consistency observed across all analytical and experimental sections of this study, supported by the experimentally validated FEA results and the posture-aware PDPS diagnostic framework, confirms the validity and practical applicability of the proposed approach for industrial multi-tasking machining centers

5. Conclusion

This study investigated the dynamic behavior of the tilt and rotation spindle head of a multitasking machining center during a change in posture, using a combination that seamlessly merges numerical and experimental approaches. The FEA code utilized for static analysis, eigenvalue analysis, and transient dynamic analysis, were performed at swing angles of either 0, 45, and 90 degrees. To verify the accuracy of the analysis results, modal analysis EMA impact hammer test experiments is conducted. The results indicate that while global maximum deformation varies by less than 1 μm across all postures, tool-point compliance and transient deformation levels are posture-sensitive, measuring 4.44 μm at 0° and 4.82 μm at 90°, and approximately 6.6 μm at 0°, 7.1 μm at 45°, and 6.4 μm at 90° respectively. The major resonance frequencies exhibit measurable posture-dependent variation, with the first natural frequency increasing from 217.8 Hz at 0° to 224.2 Hz at 90° a shift of 6.4 Hz, 2.94% while remaining focused within the 217-231 Hz band across all postures, indicating relative global dynamic stability despite the posture-dependent stiffness redistribution. On the other hand, the localized flexibilities around the cutting point and the amplitudes of the dynamic response are dependent upon the swing orientation. The deformation modes due to the swing posture as well as the transient maxima tend to emphasize the swing orientation dependence of the machining accuracy. The experimental verification of the FEA resulted in the expected range of deviations of the frequencies. There was no mode switching for the lower modes. Based on the experimentally validated structural dynamics, a PDPS was developed by integrating posture-conditioned vibration features with a posture-aware diagnostic architecture. Our results highlight the direct relationship between posture-driven dynamics and changes in the distributions of vibration features, enabling detection of deviations from the healthy vibration baseline across postures, where the healthy state corresponds to a compact feature cluster and abnormality to its dispersion relative to the GMM baseline. The spindle swing posture has minor but useful effects on structural dynamics and vibration. By embedding experimentally validated, posture-dependent structural dynamics directly into the diagnostic model, the proposed framework overcomes the posture-invariant assumption that limits conventional spindle monitoring, providing a dependable platform for resonance avoidance, precision assessment, and predictive maintenance of multi-tasking machines. Because the healthy baseline is calibrated solely from healthy-state data, the annotation-free PDPS framework requires no fault-labeled training, and its posture-stratified architecture can be extended to other multi-posture machining systems, including five-axis machining centers with tilting rotary tables and parallel kinematic machines, offering a replicable methodology for posture-aware health monitoring.

Acknowledgments

This work supported National Science and Technology Council of the R.O.C. under grants 114-2622-E-150-004 and 114-2622-E-150.

Data Availability Statement

The authors confirm that all data underlying the findings are fully available without restriction. All relevant data are within the paper.

Author Contributions

The author wrote the manuscript. The author reviewed contributed to all parts of this work.

Conflict of Interest

The authors declare no competing interests.

References

[1] W. Luo, T. Hu, Y. Ye, C. Zhang, and Y. Wei, "A hybrid predictive maintenance approach for CNC machine tool driven by Digital Twin," *Robotics and Computer-Integrated Manufacturing,* vol. 65, p. 101974, 2020, doi: https://doi.org/10.1016/j.rcim.2020.101974.

[2] W. J. Lee, H. Wu, H. Yun, H. Kim, M. B. Jun, and J. W. Sutherland, "Predictive maintenance of machine tool systems using artificial intelligence techniques applied to machine condition data," *Procedia Cirp,* vol. 80, pp. 506-511, 2019, doi: https://doi.org/10.1016/j.procir.2018.12.019.

[3] A. Voisin, T. Laloix, B. Iung, and E. Romagne, "Predictive Maintenance and part quality control from joint product-process-machine requirements: Application to a machine tool," *Procedia Manufacturing,* vol. 16, pp. 147-154, 2018, doi: https://doi.org/10.1016/j.promfg.2018.10.166.

[4] G. W. Vogl and M. A. Donmez, "A defect-driven diagnostic method for machine tool spindles," *CIRP Annals,* vol. 64, no. 1, pp. 377-380, 2015, doi: https://doi.org/10.1016/j.cirp.2015.04.103.

[5] C.-W. Lin, J. F. Tu, and J. Kamman, "An integrated thermo-mechanical-dynamic model to characterize motorized machine tool spindles during very high speed rotation," *International journal of machine tools and manufacture,* vol. 43, no. 10, pp. 1035-1050, 2003, doi: https://doi.org/10.1016/S0890-6955(03)00091-9.

[6] I. Zaghbani and V. Songmene, "Estimation of machine-tool dynamic parameters during machining operation through operational modal analysis," *International Journal of Machine Tools and Manufacture,* vol. 49, no. 12-13, pp. 947-957, 2009, doi: https://doi.org/10.1016/j.ijmachtools.2009.06.010.

[7] M. Tsutsumi and A. Saito, "Identification and compensation of systematic deviations particular to 5-axis machining centers," *International Journal of Machine Tools and Manufacture,* vol. 43, no. 8, pp. 771-780, 2003, doi: https://doi.org/10.1016/S0890-6955(03)00053-1.

[8] R. Liu, H. Wang, B. Pang, X. Gao, and H. Zong, "Load distribution calculation of a four-point-contact slewing bearing and its experimental verification," *Experimental Techniques,* vol. 42, no. 3, pp. 243-252, 2018.

[9] A. W. Khan and C. Wuyi, "Systematic geometric error modeling for workspace volumetric calibration of a 5-axis turbine blade grinding machine," *Chinese Journal of Aeronautics,* vol. 23, no. 5, pp. 604-615, 2010, doi: https://doi.org/10.1016/S1000-9361(09)60261-2.

[10] Y. Abbaszadeh-Mir, J. Mayer, G. Cloutier, and C. Fortin, "Theory and simulation for the identification of the link geometric errors for a five-axis machine tool using a telescoping magnetic ball-bar," *International Journal of Production Research,* vol. 40, no. 18, pp. 4781-4797, 2002, doi: https://doi.org/10.1080/00207540210164459.

[11] J. Mayer, Y. Mir, and C. Fortin, "Calibration of a five-axis machine tool for position independent geometric error parameters using a telescoping magnetic ball bar," in *Proceedings of the 33rd International MATADOR Conference: Formerly The International Machine Tool Desisgn and Research Conference*, 2000: Springer, pp. 275-280, doi: https://doi.org/10.1007/978-1-4471-0777-4_43.

[12] S.-H. Suh, E.-S. Lee, and S.-Y. Jung, "Error modelling and measurement for the rotary table of five-axis machine tools," *The International Journal of Advanced Manufacturing Technology,* vol. 14, no. 9, pp. 656-663, 1998, doi: https://doi.org/10.1007/BF01192286.

[13] C. Hong, C.-L. Chang, and C.-Y. Lin, "Static structural analysis of great five-axis turning–milling complex CNC machine," *Engineering Science and Technology, an International Journal,* vol. 19, no. 4, pp. 1971-1984, 2016, doi: https://doi.org/10.1016/j.jestch.2016.07.013.

[14] H. Yang, R. Zhao, W. Li, C. Yang, and L. Zhen, "Static and dynamic characteristics modeling for CK61125 CNC lathe bed basing on FEM," *Procedia engineering,* vol. 174, pp. 489-496, 2017, doi: https://doi.org/10.1016/j.proeng.2017.01.171.

[15] A. Ullah, T.-C. Chan, J.-F. Huang, and S.-L. Chang, "Finite element-integrated neural network framework for spatial modal prediction in machine tool structures," *Engineering Applications of Artificial Intelligence,* vol. 162, p. 112456, 2025, doi: https://doi.org/10.1016/j.engappai.2025.112456.

[16] A. Ullah, T.-C. Chan, and S.-L. Chang, "Current trends in vibration control and computational optimization for CNC machine tools: a comprehensive review," *The International Journal of Advanced Manufacturing Technology,* vol. 139, no. 11, pp. 5409-5444, 2025, doi: 10.1007/s00170-025-16238-8.

[17] T. M. Ericson and R. G. Parker, "Planetary gear modal vibration experiments and correlation against lumped-parameter and finite element models," *Journal of sound and vibration,* vol. 332, no. 9, pp. 2350-2375, 2013, doi: https://doi.org/10.1016/j.jsv.2012.11.004.

[18] S. N. Ganeriwala, V. Kanakasabai, A. Muthukumarasamy, T. Wolff, and M. Richardson, "Using operating deflection shapes to detect faults in rotating equipment," in *Structural Dynamics, Volume 3: Proceedings of the 28th IMAC, A Conference on Structural Dynamics, 2010*, 2011: Springer, pp. 265-271, doi: DOI
https://doi.org/10.1007/978-1-4419-9834-7_24.

[19] B. Bondsman and A. Peplow, "Experimental modal analysis and variability assessment in cross-laminated timber," *Mechanical Systems and Signal Processing,* vol. 228, p. 112466, 2025, doi: https://doi.org/10.1016/j.ymssp.2025.112466.

[20] G. W. Vogl, M. A. Donmez, and A. Archenti, "Diagnostics for geometric performance of machine tool linear axes," *CIRP annals,* vol. 65, no. 1, pp. 377-380, 2016, doi: https://doi.org/10.1016/j.cirp.2016.04.117.

[21] W. A. Smith and R. B. Randall, "Rolling element bearing diagnostics using the Case Western Reserve University data: A benchmark study," *Mechanical systems and signal processing,* vol. 64, pp. 100-131, 2015, doi: https://doi.org/10.1016/j.ymssp.2015.04.021.

[22] S. Yin, S. X. Ding, X. Xie, and H. Luo, "A review on basic data-driven approaches for industrial process monitoring," *IEEE Transactions on Industrial electronics,* vol. 61, no. 11, pp. 6418-6428, 2014, doi: DOI: 10.1109/TIE.2014.2301773.

[23] Z. Chen, C. Li, and R.-V. Sanchez, "Gearbox fault identification and classification with convolutional neural networks," *Shock and vibration,* vol. 2015, no. 1, p. 390134, 2015, doi: https://doi.org/10.1155/2015/390134.

[24] D. Jung, D. Lee, M. Kim, H. Kim, and S.-K. Park, "Mesh convergence test system in integrated platform environment for finite element analysis: D. Jung et al," *The Journal of Supercomputing,* vol. 76, no. 7, pp. 5244-5258, 2020, doi: https://doi.org/10.1007/s11227-019-02865-y

[25] F. Castellini *et al.*, "Experimental and numerical investigation of tramcar curve squeal under varying wheel-rail contact conditions," *Computers & Structures,* vol. 321, p. 108040, 2026, doi: https://doi.org/10.1016/j.compstruc.2025.108040.

[26] M. Ghadimi, R. Azarafza, A. Davar, and J. Jam, "Extraction of the descriptive function of a folding Wing with free-play using the modal test results to be used in the nonlinear motion equation of the structure," *Experimental Techniques,* vol. 49, no. 1, pp. 137-149, 2025, doi: DOI https://doi.org/10.1007/s40799-024-00734-9.

[27] P. Kumar, B. Kumar, and S. Pratap, "Experimental Exploration of Specific Wear Rate in Linear Reciprocating Motion Using Dimensional Analysis," *Experimental Techniques,* vol. 49, no. 5, pp. 949-963, 2025, doi: https://doi.org/10.1007/s40799-025-00788-3.

[28] L. Chen, J. Hong, D. Xie, and Q. Gao, "Efficient method for dynamic responses, modal and buckling analysis of cylindrical periodic structures based on the group theory and Woodbury formula," *Computers & Structures,* vol. 316, p. 107897, 2025, doi: https://doi.org/10.1016/j.compstruc.2025.107897.

[29] Z. Ming, G. Qintao, Y. Lin, and Z. Baoqiang, "Finite element model updating of jointed structure based on modal and strain frequency response function," *Journal of Mechanical Science and Technology,* vol. 33, no. 10, pp. 4583-4593, 2019, doi: DOI https://doi.org/10.1007/s12206-019-0902-0.

[30] L. Jurmu, D. Robinette, J. Blough, and C. Reynolds, "Torque Converter Dynamic Characterization Using Torque Transmissibility Frequency Response Functions: Open Clutch, Hydro-Mechanical Response," *Experimental Techniques,* vol. 49, no. 5, pp. 811-827, 2025, doi: DOI https://doi.org/10.1007/s40799-025-00777-6.

[31] S. da Silva and T. G. Ritto, "Data-driven Dirichlet sampling on manifolds for structural health monitoring," *Journal of the Brazilian Society of Mechanical Sciences and Engineering,* vol. 46, no. 7, p. 421, 2024, doi: https://doi.org/10.1007/s40430-024-04986-9

[32] F. Achouri, A. Khatir, Z. Smahi, R. Capozucca, and A. Ouled Brahim, "Structural health monitoring of beam model based on swarm intelligence-based algorithms and neural networks employing FRF," *Journal of the Brazilian Society of Mechanical Sciences and Engineering,* vol. 45, no. 12, p. 621, 2023, doi: https://doi.org/10.1007/s40430-023-04525-y

[33] M. Hamza, K. Akhtar, and M. A. Khan, "Modal and dynamic analysis of damaged steel column-beam frame structure subjected to seismic vibrations using experimental and finite element analysis approach," *Journal of the Brazilian Society of Mechanical Sciences and Engineering,* vol. 46, no. 2, p. 94, 2024, doi: https://doi.org/10.1007/s40430-023-04648-2

[34] F. B. Zahid, Z. C. Ong, and S. Y. Khoo, "A review of operational modal analysis techniques for in-service modal identification," *Journal of the Brazilian Society of Mechanical Sciences and Engineering,* vol. 42, no. 8, p. 398, 2020, doi: DOI https://doi.org/10.1007/s40430-020-02470-8.

[35] B. Clark, M. Allen, and B. Pacini, "Study of the Effect of Bolted Joint Damping-Stiffness Nonlinearity on Part Failures in Dynamic Environment Testing," *Experimental Techniques,* vol. 50, no. 1, pp. 163-174, 2026, doi: https://doi.org/10.1007/s40799-025-00827-z